



#### Article

# Time-dependent transcriptional response of tomato (Solanum lycopersicum L.) to Cu nanoparticle exposure upon infection with Fusarium oxysporum f. sp. lycopersici

Chuanxin Ma, Jaya Borgatta, Roberto De La Torre Roche, Nubia Zuverza-Mena, Jason C. White, Robert J Hamers, and Wade Elmer

ACS Sustainable Chem. Eng., Just Accepted Manuscript • Publication Date (Web): 09 May 2019

Downloaded from http://pubs.acs.org on May 9, 2019

#### **Just Accepted**

"Just Accepted" manuscripts have been peer-reviewed and accepted for publication. They are posted online prior to technical editing, formatting for publication and author proofing. The American Chemical Society provides "Just Accepted" as a service to the research community to expedite the dissemination of scientific material as soon as possible after acceptance. "Just Accepted" manuscripts appear in full in PDF format accompanied by an HTML abstract. "Just Accepted" manuscripts have been fully peer reviewed, but should not be considered the official version of record. They are citable by the Digital Object Identifier (DOI®). "Just Accepted" is an optional service offered to authors. Therefore, the "Just Accepted" Web site may not include all articles that will be published in the journal. After a manuscript is technically edited and formatted, it will be removed from the "Just Accepted" Web site and published as an ASAP article. Note that technical editing may introduce minor changes to the manuscript text and/or graphics which could affect content, and all legal disclaimers and ethical guidelines that apply to the journal pertain. ACS cannot be held responsible for errors or consequences arising from the use of information contained in these "Just Accepted" manuscripts.



# Time-dependent transcriptional response of tomato (Solanum lycopersicum L.) to Cu nanoparticle exposure upon infection with Fusarium oxysporum f. sp. lycopersici

Chuanxin Ma<sup>1</sup>, Jaya Borgatta<sup>1</sup>, Roberto De La Torre-Roche<sup>2</sup>, Nubia Zuverza-Mena<sup>2</sup>, Jason C.

White<sup>2</sup>, Robert J. Hamers<sup>1</sup>, and Wade H. Elmer<sup>3</sup>

<sup>1</sup>Center for Sustainable Nanotechnology, Department of Chemistry, University of Wisconsin, 1101 University Avenue, Madison WI 53706 USA;

<sup>2</sup> The Center for Sustainable Nanotechnology, Department of Analytical Chemistry,

The Connecticut Agricultural Experiment Station (CAES),

123 Huntington Street, New Haven, Connecticut USA;

<sup>3</sup> Center for Sustainable Nanotechnology, Department of Plant Pathology and Ecology, CAES, 123 Huntington Street, New Haven, Connecticut USA

Corresponding author Jason. White@ct.gov

Page 2 of 37

#### **ABSTRACT**

Achieving and sustaining global food security will become increasingly difficult as a changing climate increases crop loss due to greater pest and pathogen activity. Nano-enabled agrichemical delivery platforms offer a unique potential to manage pathogens and increase productivity with reduced negative environmental consequences. Two greenhouse experiments were conducted to assess the potential of in-house synthesized Cu<sub>3</sub>(PO<sub>4</sub>)<sub>2</sub>•3H<sub>2</sub>O nanosheets and commercial CuO nanoparticles (NP) to increase plant growth of tomato (Solanum lycopersicum) and suppress Fusarium oxysporum f. sp. lycopersici infection. The particles were foliarly applied once (500 mg/L; 1-2 mL dose) to seedlings prior to 30 days of growth. In control plants not treated by nanomaterials, Fusarium infection reduced plant growth by 62% across both experiments. Amendment with Cu<sub>3</sub>(PO<sub>4</sub>)<sub>2</sub>•3H<sub>2</sub>O nanosheets or CuO nanoparticles significantly reduced disease presence by an average of 31%, resulting in greater plant biomass. The time-dependent expression of three genes integral to plant defense (pathogenesis-related genes transcriptional activator [PTI5], polyphenol oxidase [PPO], and plant resistance protein 1A1 [PRP1A1]) was shown to be uniquely modulated by nanoscale Cu amendment. Specifically, Cu<sub>3</sub>(PO<sub>4</sub>)<sub>2</sub>•3H<sub>2</sub>O nanosheets increased the expression of all 3 genes in both experiments within the first 7 days of pathogen exposure, which was prior to any phenotypic evidence of disease. CuO NP showed slower increases in the genes in the plants harvested after 21 days. Importantly, these nanoscale Cu-induced changes in expression correlated well with positive changes in disease suppression and plant growth. These results highlight the importance of adequate nutrition in crop disease response and demonstrate the potential of nanoscale platforms to more effectively deliver critical micronutrients at early stages of plant development. The transcriptomic results provide important mechanistic insight into NP

Cu-based disease suppression and can be used to further optimize this important approach in nanoenabled precision agriculture.

**Keywords:** copper phosphate nanosheets; *Fusarium* root rot; foliar exposure; nanomaterial translocation; disease progress; defense-related genes

#### INTRODUCTION

The current global population is approximately 7.67 billion and is expected to increase to nearly 9.8 billion by the year 2050, with developing nations contributing the bulk of that growth. Consequently, achieving and maintaining global food security will necessitate increases in agricultural productivity by at least 70%.<sup>1, 2</sup> Unfortunately, significant negative pressure against this goal will continue to build from a changing climate, including more frequent temperature and drought extremes.<sup>3</sup> Similarly, increased activity of crop pests and pathogens due directly to an altered climate are predicted to reduce rice, wheat and maize yields by up to 25%.4 Further complicating efforts to maintain food security comes from the need for sustainability during these crop production increases, including minimal environmental impacts along with increased efficiency of water and energy inputs. Importantly, a long recognized weakness in current agricultural systems is the low efficiency of agrichemical delivery and utilization, with active ingredient losses averaging 10-75% due to processes such as leaching, degradation, and immobilization.<sup>5, 6</sup> In response, growers often over apply these materials to maintain efficacy and maximize yield. Consequently, there has been increasing interest in using nanotechnology to address these inefficiencies through novel precision agricultural approaches, with much focus on nano-formulations of traditional pesticides and fertilizers, nanosensors, and enhanced treatment of produced waste and water.6,7

Important plant micronutrients such as Cu, Mn, and Zn are known for their low *in planta* mobility and limited availability in neutral pH agricultural soils, making delivery of adequate levels of these elements to crops a problem of significant interest. In fact, nanoscale oxide forms of a number of essential plant micronutrients have been shown to positively impact plant defense and nutrition, largely through more rapid dissolution and greater availability and/or activity, which in turn led to enhanced metabolic function and growth.<sup>5,8,9</sup> Specifically, the nano-enabled delivery

of Cu has been a topic of recent active research, largely because of its multi-functionality as a key micronutrient for nutrition, a component of important plant defense pathways, and as a direct antimicrobial agent. 10, 11, 12, 13 Elmer and White demonstrated in both greenhouse and field trials that one-time foliar application of CuO NP at 100-1000 mg/L to eggplant and tomato (1-2 ml per plant) suppressed the progress of wilt disease symptoms caused by Verticillium dahliae and Fusarium oxysporum f. sp. lycopersici, respectively, by up to 69%, increased root Cu by up to 32%, and increased fresh weight by up to 64%. Importantly, this dose of Cu had no impact on the pathogens in an *in vitro* assay, suggesting that modulated innate plant defense as a function of Cu exposure resulted in the observed positive impacts. In a subsequent greenhouse study with watermelon infected by Fusarium oxysporum f. sp. niveum, Elmer et al. demonstrated that a foliar spray application of NP CuO at 500 mg/L resulted in similar reduced disease and enhanced growth.<sup>11</sup> Importantly, transcriptomic analysis of root tissues at harvest showed significant upregulation of polyphenol oxidase (PPO) and pathogenic related (PR1) genes when NP CuO and the pathogen were both present, again suggesting modulated plant defense as the mechanism of action. It is worth noting that significant concern now exists over the accumulation of Cu in terrestrial and aquatic environments<sup>14, 15</sup>; as such, the potential of nano-enabled Cu formulations to significantly lower overall application loads may confer additional benefits in terms of sustainability. For example, in a previous study we demonstrated that "tuning" nanomaterial morphology and composition could significantly impact element availability and plant response. Specifically, the effective dose of Cu<sub>3</sub>(PO<sub>4</sub>)<sub>2</sub>•3H<sub>2</sub>O nanosheets for disease control in Fusarium-infected watermelon was nearly an order of magnitude less than that of irregularly shaped CuO nanoparticles. 10

In the current study, two separate greenhouse experiments were conducted to assess the time-dependent transcriptional response of tomato upon infection with *Fusarium oxysporum* f. sp.

lycopersici and treatment with different forms of nanoscale and ionic Cu. Additional measured endpoints included biomass, disease progress, and elemental content as measured by inductively coupled plasma optical emission spectroscopy (ICP-OES) or ICP mass spectrometry (ICP-MS). For transcriptomic analysis, the expression of three genes integral to plant defense were evaluated; pathogenesis-related genes transcriptional activator (PTI5)<sup>16</sup>, polyphenol oxidase (PPO)<sup>17</sup>, and plant resistance protein 1A1 (PRP1A1). 18 The findings of this study demonstrate the enhanced efficacy of nanoscale Cu at suppressing fungal disease progress and for enhancing plant growth. In addition, the expression of key plant defense genes increased over time with infection, but was significantly modulated as a function of not only Cu amendment but also Cu type. Importantly, the changes in transcription correlated well with observed physiological and biochemical shifts in the plants. Our findings increase our understanding of the mechanisms of action for nanomaterial Cu-based disease suppression, including how chemical properties of particle dissolution, composition and morphology control activity. This work also provides useful information for the potential substitution of traditional fungicides or fertilizers, which are known to be associated with significantly environmental problems, with more sustainable materials. More importantly, these results can be used to further optimize this important approach in nano-enabled precision agriculture.

#### MATERIAL AND METHODS

**Analyte synthesis and characterization.** The CuO and  $Cu_3(PO_4)_2$  nanomaterials used in this study were a part of a larger batches also used in Borgatta et al.<sup>10</sup> Briefly,  $Cu_3(PO_4)_2 \cdot 3H_2O$  nanosheets were synthesized using a polyol method as described previously.<sup>19, 20</sup> Four mL of 2 M  $CuCl_2 \cdot 2H_2O$  were added to 20 mL of diethylene glycol followed by heating at 140 °C under reflux

for an hour. Four ml of a 3M NH<sub>4</sub>H<sub>2</sub>PO<sub>4</sub> solution was then rapidly injected and the solution was allowed to sit for 5 h. Nanosheets were then isolated by centrifugation and were rinsed with ethanol (2x) and water (1x), followed by drying overnight under vacuum. Commercial nanoscale CuO (30 nm diameter; powder) was purchased from U.S. Research Nanomaterials (Houston TX). Copper chloride dihydrate, ammonium phosphate monobasic, and diethylene glycol were obtained from Sigma Aldrich (St. Louis MO); all reagents were used as purchased. The X-ray diffraction pattern and SEM micrographs of these materials are presented in the SI for clarity. In plant exposures, the CuO and  $Cu_3(PO_4)_2 \cdot 3H_2O$  nanomaterials were applied by mass concentration (mg/L). As was previously described, the stoichiometries of CuO and  $Cu_3(PO_4)_2 \cdot 3H_2O$  result in a  $85 \pm 6\%$  and  $44 \pm 4\%$  mass percent of Cu, respectively (10). As such, each applied concentration of  $Cu_3(PO_4)_2 \cdot 3H_2O$  nanosheets had significantly less Cu than CuO nanoparticles.

Nanoparticle dissolution. Cu metal release from Cu<sub>3</sub>(PO<sub>4</sub>)<sub>2</sub>•3H<sub>2</sub>O nanosheets and CuO nanoparticles was evaluated in deionized water at pH 5.7 and 7.5, values that mimic the pH in xylem and phloem sap in plants, respectively.<sup>21</sup> The release of P from the nanosheets was also determined. Cu<sub>3</sub>(PO<sub>4</sub>)<sub>2</sub>•3H<sub>2</sub>O nanosheets and CuO nanoparticles with the equivalent amounts of Cu (0.69 mM) were prepared in 40 mL deionized water at the two different pH levels. The suspensions were sonicated for 1 min in an ultrasonic bath and then shaken at 200 rpm at ambient temperature. Samples were collected at 0.5, 1, 2, 4, 12, 24, 72, and 168 h. Three replicates were used at each time point. Ultra-centrifugal filters were used to separate particulate nanomaterials from the supernatant with the dissolved ions. The sampled supernatant was acidified with concentrated HNO<sub>3</sub> prior to analysis by ICP-MS (Agilent 7500ce).

**Plant growth experiments.** Two separate greenhouse experiments were conducted. For each, seeds of tomato (*Solanum lycopersicum* L. cv Bonnie Best; Harris Seed Co., Rochester NY) were germinated in 36 cell (5.66 x 4.93 x 5.66 cm) plastic liners (1 plant/cell) filled with soilless potting mix (ProMix BX. Premier Hort Tech, Quakertown, PA, USA). After three weeks, the seedlings were fertilized with 40 ml of Peter's soluble 20-10-20 (N-P-K) fertilizer (R.J. Peters, Inc., Allentown, PA). The pathogen inoculum was prepared as described previously. Japanese millet was autoclaved with distilled water (1:1, wt/wt) for 1 hour on two consecutive days and was seeded with three agar plugs colonized with *F. oxysporum f. sp. lycopersici Race 2*. After culture growth for 2 weeks at 22-25 °C, the millet was air-dried and ground in a mill. The inoculum was then hand incorporated into potting mix Mix BX (without mycorrhizae; Premier Hort. Tech, Quakertown, PA, USA) at 0.75 g millet inoculum/L potting mix prior to seedling addition.

Uniformly sized plants with 3-4 leaves were selected for NP exposure for each of the two separate experiments. In experiment 1, the efficacy of Cu<sub>3</sub>(PO<sub>4</sub>)<sub>2</sub>•3H<sub>2</sub>O nanosheets (500 mg/L) to suppress *Fusarium* infection was evaluated and there were four treatments; a. Untreated control, no disease b. Cu<sub>3</sub>(PO<sub>4</sub>)<sub>2</sub>•3H<sub>2</sub>O nanosheets, no disease, c. Untreated control, *Fusarium*, and d. Cu<sub>3</sub>(PO<sub>4</sub>)<sub>2</sub>•3H<sub>2</sub>O nanosheets, *Fusarium*. For experiment 2, our in-house synthesized nanosheets were compared against a commercially available CuO nanoparticles and there were 6 treatments: a. Untreated control, no disease, b. NP CuO, no disease, c. Untreated control, *Fusarium*, d. NP CuO, *Fusarium*, e. Cu<sub>3</sub>(PO<sub>4</sub>)<sub>2</sub>•3H<sub>2</sub>O nanosheets, no disease, and f. Cu<sub>3</sub>(PO<sub>4</sub>)<sub>2</sub>•3H<sub>2</sub>O nanosheets, *Fusarium*.

NP suspensions (500 mg/L) of CuO NP or Cu<sub>3</sub>(PO<sub>4</sub>)<sub>2</sub>•3H<sub>2</sub>O nanosheets were prepared in DI water amended with a nonionic surfactant (Regulaid® 1 ml/L); this type of surfactant is typical in commercial agrichemical formulations to facilitate retention to the leaves (often referred to as

"stickers"). The CuO suspension was sonicated with probe sonicator for 2 min in an ice bath. Because of concern over possible material breakage, the Cu<sub>3</sub>(PO<sub>4</sub>)<sub>2</sub>•3H<sub>2</sub>O nanosheets were sonicated using a more gentle procedure, using a bath sonicator for 1 min. A "dip application" was used for treatment; each plant was inverted into the suspension for approximately 5 seconds, resulting in a dose of approximately 1.8 mL of suspension as measured by solution volume difference before and after treatment. The plants were then inverted and allowed to drain until the foliage had completely dried (1 hour) and were then transplanted into 10 cm diameter plastic pots (350 ml) containing potting mix that was infested with *Fusarium* or not infested. We note that the solutions were re-dispersed after treatment of 5 plants. The potted plants were arranged on greenhouse benches in a randomized block design. Temperatures averaged 17-22 C° night and 19-25 C° day for the 30-d growth period. Plants were rated for severity of fungal disease on a scale of 1 to 5 where 1 = no disease, 2 = slightly stunted, 3 = stunted and or partially wilted, 4 = completely wilted, and 5 = dead. Disease progress was determined by plotting the cumulative ratings on replicate plants over time and then calculating the area-under-the-disease-progress curve (AUDPC) using the trapezoid rule: AUDPC =  $\Sigma[Y_i + Y_{(i+1)}]/2 \times (t_{(i+1)} - t_i)$ , where  $Y_i$  = the disease rating at time  $t_i$ . At harvest, the fresh shoot and root mass was separately measured and all tissues were retained for nutrient or transcriptomic analysis as described below.

**Tissue elemental analysis.** Root and foliar tissues were analyzed for elemental composition as described before.<sup>8, 10</sup> Tissues were dried in an oven at 50°C, ground in a Wiley mill, and passed through a 1 mm sieve. The ground samples (0.5 g) were added to 50 ml polypropylene digestion tubes that were amended with 5 ml of concentrated nitric acid; the samples were heated at 115 °C for 45 min using a hot block (DigiPREP System; SCP Science, Champlain, NY). After dilution,

the content of Ca, Cu, Fe, K, Mg, Mn, P, and Zn was quantified using inductively coupled plasma optical emission spectroscopy (ICP-OES) on an iCAP 6500 (Thermo Fisher Scientific, Waltham, MA). Individual element concentrations were calculated as µg/g (tissue dry mass).

Nanoparticle imaging on leaf surfaces. Suspensions of 500 mg/L Cu<sub>3</sub>(PO<sub>4</sub>)<sub>2</sub>•3H<sub>2</sub>O nanosheets or CuO nanoparticles were prepared in deionized water with the addition of several drops of Regulaid nonionic surfactant. Tomato seedlings were dipped into the nano-suspension and airdried as described above. Leaf tissues amended with Cu<sub>3</sub>(PO<sub>4</sub>)<sub>2</sub>•3H<sub>2</sub>O nanosheets or CuO nanoparticles were sampled at Day 0 and Day 7 for analysis by electron microscopy. Specifically, all samples were frozen in liquid nitrogen and then stored at -80°C until freeze-drying by a lyophilizer. The samples were then mounted on carbon sticky tape and gold coated for 90 seconds using an SPI-module sputter coater (Westchester, PA) with a discharge current of 18 mA and Ar gas. Cu<sub>3</sub>(PO<sub>4</sub>)<sub>2</sub>•3H<sub>2</sub>O nanosheet and CuO nanoparticle distribution on the leaf surface was observed using a Leo Supra V55 scanning electron microscope, with an accelerating voltage of 1 eV, and with a Thermo Scientific energy dispersive X-ray spectroscopy detector, with an accelerating voltage of 20 eV.

**Transcriptomic analysis**. In all experiments, replicate plants across all the Cu-based nanomaterial treatments were destructively harvested at three different time points during exposure; prior to visual evidence of infection, at the onset of infection, and toward the end of the exposure period when infection was at its most severe state. These time points correspond to 7, 14 and 21 d post infection. At harvest, the plant tissues were washed clean of soil, wrapped in aluminum foil, and submerged in liquid nitrogen and stored at -80°C prior to analysis for the expression of three genes

important to plant defense; polyphenol oxidase (PPO), PTI5 (a transcriptional regulator for multiple defense genes) and PR1A1 (plant resistance protein). The total RNA from 100mg of fresh root tissue was extracted with a Sigma-Aldrich Spectrum Plant Total RNA Kit (Sigma-Aldrich, St. Louis, MO). Total RNA sample quality and quantity was evaluated by a Thermo Scientific Nanodrop Lite Spectrophotometer (Thermo Fisher Scientific, Wilmington, DE) and gel electrophoresis. Two-step reverse transcription was performed on 1 µg of the extracted RNA using a Qiagen QuantiTect Reverse Transcription kit (Qiagen, Velno, The Netherlands) to synthesize the complimentary DNA (cDNA). Reverse-transcription real-time PCR (RT-qPCR) was performed with the Bio-Rad SsoAdvanced Universal SYBR Green Supermix (Bio-Rad, Hercules, CA) in an optical 96 well plate with the Bio-Rad CFX96 Touch Real-Time PCR Detection System (Bio-Rad). Briefly, the synthesized cDNA was diluted to 50 ng/μL using double distilled water. One microliter of the diluted cDNA was used as template to run the qPCR. Specific primers for each of the three selected gene transcripts were designed by Integrated DNA Technologies and the working concentration of each primer was 10 µM. The thermal profile for RT-qPCR amplifications was: 95 °C for 30 s; 95 °C for 15 s, 63 °C for 30 s, repeating 40 cycles; melting curve from 65 °C to 95 °C. A dissociation-curve step was used to confirm presence of a single amplicon in each reaction. Relative expression of each gene was estimated through  $2^{-\Delta\Delta Ct}$  method using actin of S. lycopersicum as the housekeeping gene. Gene expression was expressed relative to control plants that were not infected with F. oxysporum.

**Statistical analysis.** Biomass, elemental composition, and transcriptomic data were analyzed using one-way ANOVA with the four (experiment one) or six treatments (experiment two) as main effects. Means were separated using Tukey's Honestly Significant Difference Test at P < 0.05 or

by T-test at P < 0.05. All analyses were performed using SYSTAT V.10 (Cranes Software International Limited, Bangalore, Karnataka, India).

#### **RESULTS AND DISCUSSION**

#### **Material Characterization.**

The scanning electron micrographs and X-ray diffraction pattern are included in the supplementary information for clarity (Figure S1 and S2). Briefly, the Cu<sub>3</sub>(PO<sub>4</sub>)<sub>2</sub>•3H<sub>2</sub>O nanosheets The SEM micrographs show a sheet-like shape with lateral dimensions ranging from 50-610 nm. The crystal diffraction pattern is consistent with orthorombic Cu<sub>3</sub>(PO<sub>4</sub>)<sub>2</sub>•3H<sub>2</sub>O previously reported by Hanawalt et. al.<sup>22</sup> The CuO nanoparticles had an irregular shape, and the crystal diffraction pattern matched well with the tenorite structure.<sup>23</sup> Additional characterization data can be found in Borgatta et. al.<sup>10</sup>

#### Nanomaterial Dissolution.

The dissolution of Cu<sup>2+</sup> ions from the irregular CuO NP and Cu<sub>3</sub>(PO<sub>4</sub>)<sub>2</sub>•3H<sub>2</sub>O nanosheets was measured in deionized water at pH 5.7 and 7.5 (Figure S3). The release of Cu<sup>2+</sup> from the Cu<sub>3</sub>(PO<sub>4</sub>)<sub>2</sub>•3H<sub>2</sub>O nanosheets was rapid, with nearly 0.6 and 0.2 mg/L being released within 30 minutes at pH 5.7 and 7.5, respectively. In both instances, the rate of release had decreased markedly and remained nearly constant by 20 hours, with final release amounts of 0.95 mg/L and 0.42 mg/L at the low and higher pH values, respectively. Given the starting concentration of 0.69 mM, these final values approximate 2.2% and 0.97% dissolution at pH 5.7 and 7.5, respectively. Interestingly, the release of Cu<sup>2+</sup> from the amorphous metal oxide CuO was both slower and far less extensive than from the phosphate containing nanosheets (Figure S3). At pH 7.5, only 0.025

mg/L Cu was detected after 160 hours, corresponding to 0.057% dissolution of the CuO NPs. At pH 5.7, 0.21 mg/L Cu was dissolved from the CuO particles after 160 hours, although the data suggests that dissolution would continue for a longer period of time. Comparing across the particle types, ion dissolution was 4.8- and 17.0 times greater for the Cu<sub>3</sub>(PO<sub>4</sub>)<sub>2</sub>•3H<sub>2</sub>O nanosheets at pH 5.7 and 7.5, respectively, compared to release from the commercial CuO NPs. The faster release from the nanosheets is in agreement with that of our previous work<sup>10</sup>, where we showed that ion dissolution from Cu<sub>3</sub>(PO<sub>4</sub>)<sub>3</sub> nanosheets was shown to be nearly 3 times as rapid as dissolution from CuO nanoparticles in deionized water pH adjusted to 7.0. Importantly, that study correlated the increased rate of ion dissolution with greater suppression of fungal infection in *Citrullus lanatus* (watermelon). In the current study, the rate of P release was also measured from the nanosheets (Figure S3); the data closely match that of Cu<sup>2+</sup> release from the same material. Release values for P within the first 20 hours approached 90% of the final measured values, with greater release at the lower pH. After 160 hours, P was detected at 0.58 mg/L and 0.40 mg/L in solution, corresponding to 4.1% and 2.8% P dissolution from the nanosheets.

### **Disease Progress.**

The ability of foliarly applied copper-based nanomaterials to suppress the root fungal disease *Fusarium oxysporum f. sp. lycopersici* in tomato (*Solanum lycopersicum* L.) was investigated using a seedling dipping method (Figure 1). For the first experiment, disease progress ratings were taken 7, 14 and 21 days after treatment with 500 mg/L Cu<sub>3</sub>(PO<sub>4</sub>)<sub>2</sub>•3H<sub>2</sub>O nanosheets prior to transplanting into infested medium. The total volume of applied solution is approximately 1.8 mL, yielding a foliar Cu<sub>3</sub>(PO<sub>4</sub>)<sub>2</sub>•3H<sub>2</sub>O nanosheet dose of 0.9 mg or an elemental Cu dose of 0.4 mg/plant. Assessing disease progress involved calculating the area under the disease progress

curve (AUDPC), with lower values representing less disease progression and plant damage. Figure 2a shows disease progress for the three harvests; at 7 d, no disease was evident in the control or nanosheet-amended plants. By harvest 2 (14 d), disease was significant in the untreated controls but the Cu<sub>3</sub>(PO<sub>4</sub>)<sub>2</sub>•3H<sub>2</sub>O nanosheet-treated plants showed minimal signs of infection and were statistically equivalent to non-infected controls, demonstrating that the nanosheets significantly slowed the onset of disease. By harvest 3 (21 d), disease was also evident in the Cu<sub>3</sub>(PO<sub>4</sub>)<sub>2</sub>•3H<sub>2</sub>O nanosheet-treated plants, although the level of infection was significantly less (32%) than untreated infected controls. Figure 2b shows the AUDPC data normalized to the un-infected controls at each harvest and then the data were pooled (time points were collapsed since all data was expressed relative to 1.0). In this pooled data, Cu<sub>3</sub>(PO<sub>4</sub>)<sub>2</sub>•3H<sub>2</sub>O nanosheet-treated plants exhibited 42% less disease than the *Fusarium* controls and were statistically equivalent to non-treated un-infected controls. The data show that foliar application of Cu<sub>3</sub>(PO<sub>4</sub>)<sub>2</sub>•3H<sub>2</sub>O delayed the disease onset until the third harvesting period, indicating enhanced initial plant defense.

In the second experiment, commercial CuO NP were included for comparison. Disease progress ratings were taken 7, 14, 21, and 28 days after transplanting into the infested medium (Figure 3a). At harvest one, there was no evidence of disease in the 3 infected treatments but by harvest 2, both the control and Cu<sub>3</sub>(PO<sub>4</sub>)<sub>2</sub>•3H<sub>2</sub>O-nanosheet-treated plants showing significant symptoms of infection. Importantly, the progress of disease upon nanosheet treatment was significantly reduced (33-38%) compared to that of the infected controls, and in the CuO NP treatment, there was no statistically significant evidence of disease at all. These findings align with those of experiment 1, demonstrating that copper-based nanomaterials can significantly slow the progress of disease. By harvest 3 and 4, disease had continued to progress in the controls, but at both intervals, treatment with both CuO NPs and Cu<sub>3</sub>(PO<sub>4</sub>)<sub>2</sub>•3H<sub>2</sub>O nanosheets had significantly

reduced disease progress by 22-33%, although there was no difference in efficacy between the two types of Cu. Figure 3b shows the AUDPC data normalized to the uninfected control values at each harvest and then pooled across all time points; again, it is clear that single foliar applications of either type of Cu nanomaterial at the seedling stage significantly reduced *Fusarium* disease progress during the following weeks of growth.

There has been significant interest in the use of nanoscale materials to suppress crop pathogens in agriculture<sup>6, 12</sup>, often involving materials that are antimicrobial and act directly on the agent of concern. For example, Graham et al. evaluated two different forms of nanoscale zinc oxide for the direct control of *Xanthomonas citri*, the pathogen responsible for citrus canker.<sup>24</sup> The authors reported that the minimum inhibitory concentration was two-fold lower for nanoscale zinc products than for traditional bactericides. Similarly, Strayer-Scherer et al. showed in both *in vitro* assays and a greenhouse study that a number of copper nanomaterials were more effective at reducing the growth and damage caused by *Xanthomonas perforans*, than were traditional pesticides.<sup>13</sup> Both Huang et al. and Liao et al. showed that nanoscale Mg had notable efficacy against bacterial plant pathogens.<sup>14, 25</sup> In addition, Hao et al demonstrated that several carbon-based and metal oxide nanomaterials inhibited viral pathogen infection, including Turnip Mosaic virus in tobacco and *Podosphaera pannosa* in rose.<sup>26, 27</sup>

However, the current study is focused on suppressing fungal infection through modulation of plant nutrition and plant defense.<sup>28</sup> It is known that micronutrients such as Cu are critical to plant defensive pathways, particularly in the roots for soil-borne pathogens<sup>29,30</sup>, but the availability of these materials in soil is often low due to pH-induced precipitation<sup>31</sup> and basipetal transport is limited<sup>32</sup>, confounding the potential for foliar application.<sup>12,28</sup> Given the known enhanced activity and greater *in planta* transport of materials at the nanoscale, a number of recent studies from our

group and others have focused on nanoparticle micronutrients for enhanced nutrition and disease suppression. By adapting a well-established strategy of foliar feeding with macronutrients<sup>33</sup>, Elmer and White demonstrated that foliarly applied nanoscale CuO, MnO, or ZnO in both greenhouse and field studies all slowed the disease progress of *Fusarium* in tomato and *Verticillium* in eggplant more effectively the corresponding bulk fertilizers.<sup>8</sup> Importantly, the authors reported that neither the CuO nor MnO were inhibitory to the pathogen in an *in vitro* assay at the concentrations used in the study. Similar nutritionally modulated disease suppression activity was reported in greenhouse and field trials with nanoscale Cu in different forms for *Fusarium* wilt in watermelon caused by *F. oxysporum* f. sp. *niveum*.<sup>10, 11</sup> Interestingly, Adisa et al. showed that in greenhouse studies, nanoceria (50 mg/L), which is not a required nutrient, suppressed *Fusarium* infection in tomato.<sup>34</sup> Although the mechanism is not entirely clear, enhanced photosynthetic potential, as well as increased catalase and PPO activity, were reported with Ce amendment.

#### **Biomass**

For the first experiment, the total root, shoot and plant biomass was recorded at destructive harvests 7, 14, and 21 d after transplanting to infested media. At harvest 1, the root, shoot and total biomass of the uninfected control and nanosheet groups were 1.8, 7.3, 9.11 g (wet mass) and 1.7, 7.4, and 9.0 g, respectively (Table S1). For the infected controls, these values were non-significantly reduced at 1.3, 5.0 and 6.3g, respectively, but for the infected nanosheet-treated plants, root, shoot and total we mass values were significantly reduced at 1.3, 4.1 and 5.4 g, respectively. For the uninfected plants, the mass of each tissue and the total mass doubled by the second harvest and increased marginally by the third harvest, with root, shoot and total mass values ranging from 5.1-8.9, 12.1-13.4, and 18.5-21.0 g, respectively. Upon fungal infection, the tissue and total

biomass of the tomato were significantly reduced by 54-66% to values of 2.3-2.4, 3.9-4.2, and 6.3-8.6 g, respectively; again, treatment with the nanosheets had no impact on plant biomass. By harvest 3, reductions in plant mass for the untreated controls continued to worsen, with total plant mass averaging only 6.7 g; importantly, the nanosheet treated plants had total biomass values of 13.7 g, demonstrating that Cu<sub>3</sub>(PO<sub>4</sub>)<sub>2</sub>•3H<sub>2</sub>O nanosheet significantly suppressed the negative effects of disease. Figure 4A shows the total plant biomass of tomato at the three harvests, with the data in each harvest being normalized to the non-infected controls at the first harvest. Reductions of 31-41% in total biomass with disease were evident in both control and Cu<sub>3</sub>(PO<sub>4</sub>)<sub>2</sub>•3H<sub>2</sub>O nanosheet-treated plants by the second harvest, and at that point, amendment with the nanomaterial had no effect. However, by the final harvest, infection reduced plant mass by 67% relative to the controls but in the nanosheet-treated plants, the reduction with disease was reduced by only 34%, indicating the level of infection was reduced by half with early Cu<sub>3</sub>(PO<sub>4</sub>)<sub>2</sub>•3H<sub>2</sub>O nanosheet treatment.

For experiment 2, the shoot, root, and total mass of select harvested plants was determined 7, 14, and 21 d after transplanting to infested media. At harvest 1, the root, shoot and total biomass of the plants was largely unaffected by infection or treatment, with root, shoot and total biomass ranging from 1.9-3.2, 2.5-6.2, and 4.4-7.3 g, respectively (Table S2). By harvest 2, the average root and shoot biomass for the infected controls were significantly reduced; values in the untreated uninfected controls were 3.9, 10.9 and 14.7 g, respectively, but the infected plant values were 2.9, 4.8, and 7.8 g, respectively. The biomass of plants in the CuO NPs and Cu<sub>3</sub>(PO<sub>4</sub>)<sub>2</sub>•3H<sub>2</sub>O nanosheet treatments were statistically equivalent and more importantly, were not affected by disease; values for the roots, shoots and total mass ranged from 3.8-5.2, 6.6-9.8, and 10.4-15.1 g, respectively. At the third harvest, biomass of the infected plants was unchanged from harvest two (3.0, 4.6, and 7.6 g for roots, shoots, and total mass, respectively) as compared to 5.5, 11.9, and 17.1 g for the un-

infected controls, respectively. Similarly, the biomass of the Cu<sub>3</sub>(PO<sub>4</sub>)<sub>2</sub>•3H<sub>2</sub>O nanosheet-treated plants had not increased at harvest 3 but for the CuO NPs-treated plants, the biomass had continued to increase significantly, regardless of disease, with values ranging from 5.3-7.3, 9.9-15.1, and 15.2-22.4 g for roots, shoots, and total mass, respectively.

The normalized biomass data are shown in Figure 4B; here, all data was expressed relative to the total plant mass of the uninfected, untreated controls at the 7-d harvest. At harvest 1, there was a trend for reduced total biomass with infection in the control and two Cu treatments, although the reduction was statistically significant for the Cu<sub>3</sub>(PO<sub>4</sub>)<sub>2</sub>•3H<sub>2</sub>O nanosheet-treated plants. At harvest 2, disease had reduced the biomass of infected control plants by 47%; however, the CuO NPs and Cu<sub>3</sub>(PO<sub>4</sub>)<sub>2</sub>•3H<sub>2</sub>O treated plants had biomass that was statistically equivalent to their respective un-infected controls. These findings align with the disease data from this experiment and again demonstrate the efficacy of Cu-based nanomaterials at slowing the onset of disease early stage upon foliar treatment. By the third harvest, infection had reduced plant biomass by 57% and the benefit of Cu<sub>3</sub>(PO<sub>4</sub>)<sub>2</sub>•3H<sub>2</sub>O nanosheet treatment had been lost, with these plants having biomass that was 49% that of the controls. However, the CuO NPs treated plants had statistically equivalent biomass to the uninfected controls.

It is clear that the slowed onset of disease afforded by early life stage nanoscale Cu amendment clearly resulted in enhanced growth; these findings are supported by a number of recent studies in the literature. Elmer and White reported that a nanoscale CuO (same material as the current study) foliar application to seedlings increased tomato biomass by 33% upon infection by *F. oxysporum* f. sp *lycopersici* and increased eggplant biomass by 34% upon infection with *V. dahlia*. Borgatta et al. reported that *Fusarium* infection reduced watermelon biomass by 80%, but that both commercial CuO NPs and Cu<sub>3</sub>(PO<sub>4</sub>)<sub>2</sub>•3H<sub>2</sub>O nanosheets increased watermelon growth by

up to 100%; notably, the nanosheets were effective at a 10-fold lower dose than the commercial CuO nanoparticles and this effect seemed to be related to differences in chemical composition, as well as perhaps morphological differences, that resulted in faster dissolution. 10 Elmer at al. reported that in six of eight greenhouse experiments, foliar application of CuO nanoparticles at 500 mg/L (1-2 mL total volume) increased watermelon growth, including 39-53% more fruit in two field studies conducted in 2016 and 2017.<sup>11</sup> In previous studies, it is notable that single applications of these nanomaterials at the seedling stage provides life cycle-long positive impacts on growth and disease. Interestingly, Borgatta et al. were able to correlate greater Cu<sup>2+</sup> dissolution from the nanosheets with enhanced disease suppression and growth in fungus-infected watermelon. 10 Although the dissolution data was confirmed in the current study, the relationship between more rapid ion release from the nanosheets relative to commercial CuO nanoparticles and disease suppression or plant biomass was less definitive than observed in our previous study. The reasons for this difference are not entirely clear but could be related to different species of both the fungal pathogen and the host crop. Notably, additional investigations on seed treatments and multiple applications during growth are currently underway.

#### Elemental analysis.

The elemental content of harvested root and shoot tissues was determined by ICP-OES or ICP-MS. In experiment 1, there were few consistent trends in the levels of the 14 measured elements as a function of treatment or harvest time (Table S3). The concentration of Cu in the roots of harvested plants did not vary significantly by treatment or harvest time and ranged from 10-45 mg/kg. However, the Cu shoot of Cu<sub>3</sub>(PO<sub>4</sub>)<sub>2</sub>•3H<sub>2</sub>O nanosheet treated plants was expectedly higher (given the foliar application), with levels at the first harvest being 160-180 mg/kg as compared to

8-10 mg/kg in the control plants. In the treated plants, there was a time-dependent decrease in Cu levels to the third harvest, when concentrations ranged from 16-57 mg/kg. This decrease in content is likely a function of growth dilution (new biomass not directly exposed to the nanosheets). The root Cu content for the plants did not differ significantly across harvests or with treatment. The average Cu content of all plants, regardless of disease or harvest, not receiving foliar Cu amendment was 23.6 mg/kg (±2.78); the value for Cu<sub>3</sub>(PO<sub>4</sub>)<sub>2</sub>•3H<sub>2</sub>O nanosheet-amended plants was 31.3 mg/Kg (±4.70). Although there is a trend of increased root Cu content, the values are not significantly different. It is also interesting to note that disease, regardless of Cu treatment, tended to increase Zn, Mn and P content (10-60%) in the roots and shoots of the tomato plants.

In experiment 2, the same elements were analyzed and the overall trend was consistent; although some elements did vary across treatments, there were few consistent or discernable patterns in the data (Tables S4-S8). Similar to experiment 1, the concentration of Cu in the roots of all plants ranged from 10-30 mg/Kg. As expected, the Cu shoot content of plants receiving foliar Cu amendment was greater than the controls, ranging from 40-100 mg/kg, depending on the treatment and as in experiment 1, this amount decreased with time (to 10-30 mg/kg) with growth dilution. Interestingly, at the first harvest, the amount of Cu in the shoots of plants receiving the Cu<sub>3</sub>(PO<sub>4</sub>)<sub>2</sub> nanosheets (averaging 107 mg/kg) was significantly greater than that of the plants exposed to CuO NPs (45.9 mg/k). Importantly, Cu<sub>3</sub>(PO<sub>4</sub>)<sub>2</sub> nanosheets yield higher Cu concentration in the roots despite the fact that when expressed as elemental Cu, the CuO treated plants received twice as much Cu as the Cu<sub>3</sub>(PO<sub>4</sub>)<sub>2</sub> nanosheets. Although reason for the different foliar Cu levels are not known, we anticipate that the flake-like shape of Cu<sub>3</sub>(PO<sub>4</sub>)<sub>2</sub> nanosheets likely enhances binding to the leaf surfaces, while composition-dependent differences in dissolution rate and subsequent Cu<sup>2+</sup> ion uptake between Cu<sub>3</sub>(PO<sub>4</sub>)<sub>2</sub> and CuO also likely play a

role. Also, similar to the first experiment, there were time-dependent increases in Zn and Mn content, although the trends were weaker in the second trial. Conversely, the results for P content in the plants across the two experiments is more definitive (Figure S4). Regardless of Cu treatment, the P content in both root and shoot tissues was significantly increased upon *Fusarium* infection. Interestingly, this effect was qualitatively time dependent, with infected plants having 2.14 times more P in their tissues by the final harvest of both experiments.

Given that the proposed mode of action for Cu-induced disease suppression is related to improved crop nutrition, an assessment of element/nutritional content is important. Our current interest in using foliarly applied nanoscale Cu to treat root disease arose from the work of Wang et al., where increased root Cu was detected after foliar application of nanoparticle CuO in maize and most importantly, this was not observed with non-nanoscale forms of the element.<sup>35</sup> However, work to date has been mixed with regard to the detection of enhanced Cu in the roots of exposed plants after foliar application. Elmer and White did detect increased root Cu in tomato and eggplant treated with nanoscale CuO and this enhanced level of Cu correlated well with less disease and increased biomass in both greenhouse and field trials. Similarly, Elmer et al. reported significantly increased Cu in the roots of treated watermelon plants from a greenhouse experiment but did note that in field trials, the harvested fruit had Cu concentrations that were equivalent to the untreated controls.<sup>11</sup> Conversely, Borgatta et al. did not detect increased Cu in the roots of treated watermelon<sup>10</sup>; these findings align with those of our current study, although the non-statistically significant trend did suggest potential increased root Cu. The reasons for this variability in our studies is unclear but could be a function of plant species, extent of infection, growth conditions, timing of application or other unforeseen factors. As such, more in-depth molecular analysis such as that below will likely be necessary to elucidate key mechanisms of action. With regard to shoot Cu data, the significantly greater element content for the Cu<sub>3</sub>(PO<sub>4</sub>)<sub>2</sub>•3H<sub>2</sub>O nanosheets when compared to CuO nanoparticles is particularly interesting. When adjusted for elemental Cu, the nanosheets led to about a 4-fold increase in residual Cu on or in the shoots. Clearly additional work is needed to determine the distribution of this additional Cu on or in the shoot system but it is apparent that the excess levels did not correlate with increased suppression of disease or transfer to the root tissues. Borgatta et al. reported no difference in the shoot content of Cu for watermelon treated with these two materials <sup>10</sup>, although in that study tissues were only analyzed at the end of the growth period. However, one finding from that study clearly implicated particle morphology and composition as key factors in the observed plant and pathogen response; the findings of the current study seem to support that conclusion. In looking at the other elements in the root and shoot tissues, there appeared to be few consistent trends in the data as a function of treatment. Clearly, plant metabolic function as a consequence of disease and of nutritional amendment are complex processes and more detailed study will be necessary to understand these processes.

# Nanoparticle imaging on leaf surfaces.

Figure 5 shows SEM images of Cu<sub>3</sub>(PO<sub>4</sub>)<sub>2</sub>•3H<sub>2</sub>O nanosheets and CuO nanoparticles on the surface of tomato leaves; with samples collected on the day of exposure and 7 days after initial application. There were no overt qualitative differences in the nanomaterial amount or distribution on the leaf surfaces between 0 and 7 days after application. The Cu<sub>3</sub>(PO<sub>4</sub>)<sub>2</sub>•3H<sub>2</sub>O nanosheets appear to dry in aggregates that lay flat on the leaf surface, while the CuO nanoparticles seem to be more sparsely distributed across the leaf surface. For both nanomaterials, the particles were observed close to or even in contact with structures such as stomata and trichomes (Figure 5). Given that the actual mechanism of particle entry into the leaf is currently unknown, these images

are instructive but not conclusive. Additional SEM images with associated EDS analysis can be found in the SI (Figure S5 and Figure S6).

# Transcriptomics.

Gene expression analysis was conducted on the root tissues of plants from the two experiments to investigate the impact of disease and of Cu nanomaterial amendment on the transcription of three genes integral to plant defense; PPO, PTI5, and PR1A1. In the first experiment, the expression of these genes was evaluated at 7 and 14 d after transplanting into infested soil (Figure 6A). The transcription of PPO, PTI5, and PR1A1 in the two sets of uninfected plants, both no treatment and amendment with nanosheets, showed relatively consistent levels of expression across the two time points. Similarly, in the Fusarium-infected controls, PPO expression was unchanged over the two sampling periods and not significantly different from the controls. The expression of PR1A1 was increased by 7-fold at the first harvest, although levels decreased to 5-fold that of controls in the second harvest. Alternatively, the expression of PTI5 was unchanged at the first harvest but by 14 d post transplanting to infested media, the value had increased to 10-fold that of the non-infected controls. Notably, Cu<sub>3</sub>(PO<sub>4</sub>)<sub>2</sub>•3H<sub>2</sub>O nanosheet treatment increased the expression of PPO, PTI5, and PR1A1 by 10-40 fold in Fusarium-infected plants. It is important to note that this significant increase in the expression of plant defense genes occurred prior to phenotypic evidence of disease and correlated well with increased biomass at the later time points.

In experiment two, the expression of PPO, PTI5, and PR1A1 was determined in plants harvested 7, 14, and 21 d after transplanting into infested or non-infested potting media and is shown in Figure 6B. In the uninfected plants, the expression of PPO was unchanged across all time

points and for the two Cu-based materials. However, the expression of PTI5 in the un-infected plants increased significantly from harvest periods 1-3; the reasons for this are currently under investigation. Conversely, in the uninfected controls, the expression of PR1A1 decreased across the control and two Cu nanomaterial treatments. Importantly, similar to experiment 1, treatment of the plants with Cu<sub>3</sub>(PO<sub>4</sub>)<sub>2</sub>•3H<sub>2</sub>O nanosheets significantly increased the expression levels (2.5 to 5-fold) of PPO, PTI5, and PR1A1 at harvest 1. For PPO, the expression level decreased significantly at the latter two harvests; for PTI5 and PR1A1, the levels upon treatment with Cu<sub>3</sub>(PO<sub>4</sub>)<sub>2</sub>•3H<sub>2</sub>O nanosheet were constant or of similar magnitude in the latter two harvests. CuO exposure in the infected plants resulted in a time-dependent increase in expression of all three genes. At harvest 1 and 2, levels were equivalent to and slightly increased from the untreated control plants but at harvest 3, the expression was significantly greater for each of the genes (1.5 to 2.5-fold). These findings align with the results from the disease progress and biomass determinations, indicating the copper nanomaterial exposure stimulated plant defensive response which resulted in greater overall health and growth in the presence of the pathogen. Notably, in the untreated but infected control plants, expression of the three genes tended to increase with harvest time as well, although this reactive increase appears to be more delayed and did not translate to significant level of disease suppression.

There is little work published on the transcriptomic response of pathogen-impacted plants to nanoscale nutrients as a strategy to promote plant health. It has been known for decades that a number of micronutrients are critical to plant defense and secondary metabolite pathways and that supplying adequate levels of these nutrients to plants is difficult. Given what is known about the enhanced availability, reactivity, and *in planta* translocation of nanoscale materials, it is not surprising that such amendments could positively impact plant metabolism and physiology,

thereby reducing the negative impacts of pathogen infection.<sup>6</sup> In the current study, the transcription of 3 genes critical to plant health and disease response; PPO, PTI5, and PR1A1, were all significantly upregulated in the root tissue upon nanoscale Cu treatment. This early life stage influx of Cu and the resulting molecular response led directly to increased growth and reduced disease presence. These findings align well with Elmer et al., where the authors demonstrated up regulation of PPO and PR1A1 in watermelon shoots that were infected with *Fusarium* but also treated with foliar CuO NPs.<sup>11</sup> The current study demonstrates the important time-dependent nature of this response, both in terms of understanding the mechanisms of action but also for efforts at optimizing management strategies. These findings could have far reaching impacts on agricultural systems. Single nanoscale Cu applications to young plants could feasibly be used to initiate inherent production of a cascade of host defense products to proactively protect plants and positively impact crop yield under biotically or abiotically stressed conditions.

#### Conclusions.

In summary, in-house synthesized Cu<sub>3</sub>(PO<sub>4</sub>)<sub>2</sub>•3H<sub>2</sub>O nanosheets and commercial CuO nanoparticles (NP) were applied to young tomato seedlings prior to subsequent growth in potting media infested with the fungal pathogen *Fusarium oxysporum* f. sp. *lycopersici* in two greenhouse studies. Although fungal infection reduced plant biomass by 62%, foliar nanoscale Cu treatment at the seedling stage reduced disease severity by 31% and promoted overall plant biomass. Importantly, both nanomaterials yielded a time-dependent transcriptional increase of a number of plant defense genes, with the Cu<sub>3</sub>(PO<sub>4</sub>)<sub>2</sub>•3H<sub>2</sub>O nanosheets exerting that impact prior to any phenotypic evidence of disease. The findings demonstrate that manipulation of crop nutrition with required micronutrients in nanoscale form has significant potential as an effective and sustainable

disease management strategy. A mechanistic understanding of these processes at the transcriptomic level will be critical to optimizing this approach. Future work is focused on the timing and potential of multiple nanoscale amendments, as well as on tuning the synthesis of these materials with regard to morphology, physical characteristics or surface functionality to maximize disease suppression activity. Such strategies have the potential to be an important tool in efforts to achieving and maintaining global food security.

#### ASSOCIATED CONTENT

# **Supporting information**

The Supporting Information is available free of charge on the ACS Publications website at DOI: XXXXX.

Additional information on SEM images and X-ray diffraction patterns of Cu-based nanomaterials, time-dependent Cu<sup>2+</sup> dissolution from both Cu-based nanomaterials, the P content in tomato shoots and roots, macro- and micro-nutrient content in tomato shoots and roots, SEM images of Cu-based nanomaterial distribution on the leaf surface and the corresponding EDS maps (PDF).

#### **ORCID**

Chuanxin Ma: 0000-0001-5125-7322

Jaya Borgatta: 0000-0002-9381-6097

Roberto De La Torre-Roche: 0000-0001-7370-4373

Nubia Zuverza-Mena: 0000-0003-2721-7691

Jason C. White: 0000-0001-5001-8143

Robert J. Hamers: 0000-0003-3821-9625

Wade H. Elmer: 0000-0003-3308-4899

# Acknowledgements.

This work was supported by the National Science Foundation under the Center for Sustainable Nanotechnology, CHE-1503408. The CSN is part of the Centers for Chemical Innovation Program. ICP-OES and ICP-MS work done by RDLTR and NZM was supported by USDA-NIFA-AFRI 2016-67021-24985 and FDA 1U18FD005505-04, respectively. We also thank Mr. Peter Thiel for technical assistance.

#### References

- 1. Nations, U. World Population Prospects: The 2015 Revision, Key Findings and Advance Tables; Department of Economics and Social Affairs, Population Division: 2015.
- 2. Rodrigues, S. M.; Demokritou, P.; Dokoozlian, N.; Hendren, C. O.; Karn, B.; Mauter, M. S.; Sadik, O. A.; Safarpour, M.; Unrine, J. M.; Viers, J., Nanotechnology for sustainable food production: promising opportunities and scientific challenges. *Environmental Science: Nano* **2017**, *4* (4), 767-781, DOI 10.1039/C6EN00573J
- 3. (IPCC), I. P. o. C. C. Global warming of 1.5 oC. https://www.ipcc.ch/sr15/. .
- 4. Deutsch, C. A.; Tewksbury, J. J.; Tigchelaar, M.; Battisti, D. S.; Merrill, S. C.; Huey, R. B.; Naylor, R. L., Increase in crop losses to insect pests in a warming climate. *Science* **2018**, *361* (6405), 916-919, DOI 10.1126/science.aat3466
- 5. Servin, A.; Elmer, W.; Mukherjee, A.; De la Torre-Roche, R.; Hamdi, H.; White, J. C.; Bindraban, P.; Dimkpa, C., A review of the use of engineered nanomaterials to suppress plant disease and enhance crop yield. *J Nanopart Res* **2015**, *17* (2), 92, DOI 10.1007/s11051-015-2907-7
- 6. White, J. C.; Gardea-Torresdey, J., Achieving food security through the very small. *Nature nanotechnology* **2018**, *13* (8), 627, DOI 10.1038/s41565-018-0223-y
- 7. Kah, M.; Kookana, R. S.; Gogos, A.; Bucheli, T. D., A critical evaluation of nanopesticides and nanofertilizers against their conventional analogues. *Nature nanotechnology* **2018**, *13* (8), 677, DOI 10.1038/s41565-018-0131-1
- 8. Elmer, W. H.; White, J. C., The use of metallic oxide nanoparticles to enhance growth of tomatoes and eggplants in disease infested soil or soilless medium. *Environmental Science: Nano* **2016,** *3* (5), 1072-1079, DOI 10.1039/C6EN00146G
- 9. Dimkpa, C.; Singh, U.; Adisa, I.; Bindraban, P.; Elmer, W.; Gardea-Torresdey, J.; White, J., Effects of manganese nanoparticle exposure on nutrient acquisition in wheat (Triticum aestivum L.). *Agronomy* **2018**, *8* (9), 158, DOI 10.3390/agronomy8090158
- 10. Borgatta, J.; Ma, C.; Hudson-Smith, N.; Elmer, W.; Plaza Pérez, C. D.; De La Torre-Roche, R.; Zuverza-Mena, N.; Haynes, C. L.; White, J. C.; Hamers, R. J., Copper Based Nanomaterials Suppress Root Fungal Disease in Watermelon (Citrullus lanatus): Role of Particle Morphology, Composition and Dissolution Behavior. *ACS Sustainable Chemistry & Engineering* **2018**, *6* (11), 14847-14856, DOI 10.1021/acssuschemeng.8b03379
- 11. Elmer, W.; De La Torre-Roche, R.; Pagano, L.; Majumdar, S.; Zuverza-Mena, N.; Dimkpa, C.; Gardea-Torresdey, J.; White, J. C., Effect of metalloid and metal oxide nanoparticles on Fusarium wilt of watermelon. *Plant disease* **2018**, *102* (7), 1394-1401, DOI 10.1094/PDIS-10-17-1621-RE
- 12. Elmer, W.; White, J. C., The future of nanotechnology in plant pathology. *Annual review of phytopathology* **2018**, *56*, 111-133, DOI 10.1146/annurev-phyto-080417-050108
- 13. Strayer-Scherer, A.; Liao, Y.; Young, M.; Ritchie, L.; Vallad, G.; Santra, S.; Freeman, J.; Clark, D.; Jones, J.; Paret, M., Advanced copper composites against coppertolerant Xanthomonas perforans and tomato bacterial spot. *Phytopathology* **2018**, *108* (2), 196-205, DOI doi.org/10.1094/PHYTO-06-17-0221-R
- 14. Liao, Y.-Y.; Strayer-Scherer, A.; White, J.; Mukherjee, A.; De La Torre-Roche, R.; Ritchie, L.; Colee, J.; Vallad, G.; Freeman, J.; Jones, J., Nano-Magnesium Oxide: A Novel Bactericide Against Copper-Tolerant Xanthomonas perforans Causing Tomato Bacterial Spot. *Phytopathology* **2018**, *109* (1), 52-62, DOI doi.org/10.1094/PHYTO-05-18-0152-R

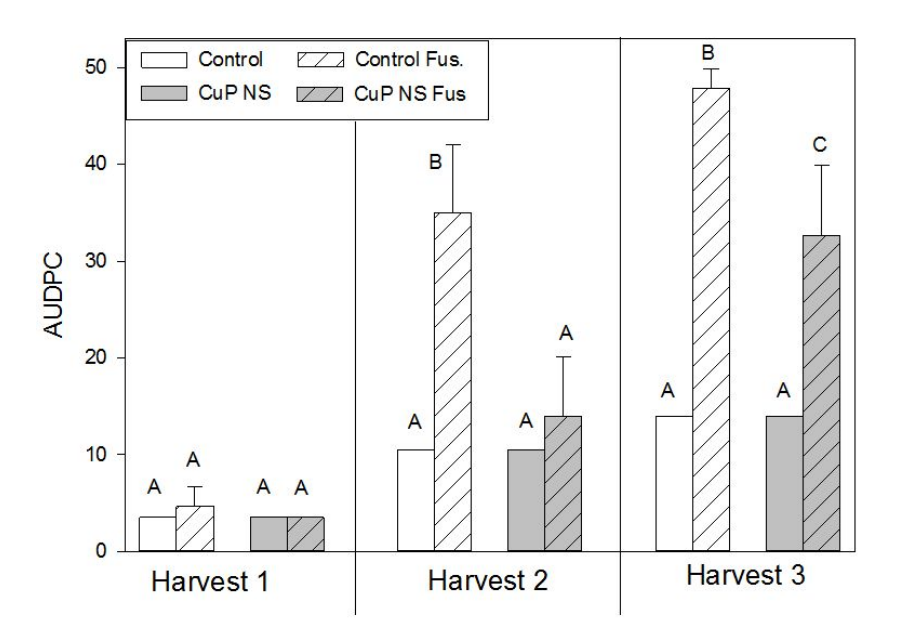
- 15. Pietrzak, U.; McPhail, D., Copper accumulation, distribution and fractionation in vineyard soils of Victoria, Australia. *Geoderma* **2004**, *122* (2-4), 151-166, DOI 10.1016/j.geoderma.2004.01.005
- 16. He, P.; Warren, R. F.; Zhao, T.; Shan, L.; Zhu, L.; Tang, X.; Zhou, J.-M., Overexpression of Pti5 in tomato potentiates pathogen-induced defense gene expression and enhances disease resistance to Pseudomonas syringae pv. tomato. *Molecular plant-microbe interactions* **2001**, *14* (12), 1453-1457, DOI 10.1094/MPMI.2001.14.12.1453
- 17. Li, L.; Steffens, J. C., Overexpression of polyphenol oxidase in transgenic tomato plants results in enhanced bacterial disease resistance. *Planta* **2002**, *215* (2), 239-247, DOI 10.1007/s00425-002-0750-4
- 18. Veluchamy, S.; Panthee, D. R., Differential expression analysis of a select list of genes in susceptible and resistant heirloom tomatoes with respect to Pseudomonas syringae pv. tomato. *European journal of plant pathology* **2015**, *142* (4), 653-663, DOI 10.1007/s10658-015-0621-z
- 19. Kim, D.-H.; Kim, J., Synthesis of LiFePO4 nanoparticles in polyol medium and their electrochemical properties. *Electrochemical and Solid-State Letters* **2006**, *9* (9), A439-A442, DOI **10.1149/1.2218308**
- 20. Wang, D.; Buqa, H.; Crouzet, M.; Deghenghi, G.; Drezen, T.; Exnar, I.; Kwon, N.-H.; Miners, J. H.; Poletto, L.; Grätzel, M., High-performance, nano-structured LiMnPO4 synthesized via a polyol method. *Journal of Power Sources* **2009**, *189* (1), 624-628, DOI 10.1016/j.jpowsour.2008.09.077
- 21. Hijaz, F.; Killiny, N., Collection and chemical composition of phloem sap from Citrus sinensis L. Osbeck (sweet orange). *PloS one* **2014,** *9* (7), e101830, DOI 10.1371/journal.pone.0101830
- 22. Hanawalt, J.; Rinn, H.; Frevel, L., Chemical analysis by X-ray diffraction. *Industrial & Engineering Chemistry Analytical Edition* **1938**, *10* (9), 457-512.
- 23. Åsbrink, S.; Norrby, L.-J., A refinement of the crystal structure of copper (II) oxide with a discussion of some exceptional esd's. *Acta Crystallographica Section B: Structural Crystallography and Crystal Chemistry* **1970**, *26* (1), 8-15, DOI 10.1107/S0567740870001838
- 24. Graham, J.; Johnson, E.; Myers, M.; Young, M.; Rajasekaran, P.; Das, S.; Santra, S., Potential of nano-formulated zinc oxide for control of citrus canker on grapefruit trees. *Plant disease* **2016**, *100* (12), 2442-2447, DOI 10.1094/PDIS-05-16-0598-RE
- 25. Huang, Z.; Rajasekaran, P.; Ozcan, A.; Santra, S., Antimicrobial Magnesium Hydroxide Nanoparticles As an Alternative to Cu Biocide for Crop Protection. *Journal of agricultural and food chemistry* **2018**, *66* (33), 8679-8686, DOI 10.1021/acs.jafc.8b01727
- 26. Hao, Y.; Yuan, W.; Ma, C.; White, J. C.; Zhang, Z.; Adeel, M.; Zhou, T.; Rui, Y.; Xing, B., Engineered nanomaterials suppress Turnip mosaic virus infection in tobacco (Nicotiana benthamiana). *Environmental Science: Nano* **2018**, *5* (7), 1685-1693, DOI 10.1039/C8EN00014J
- 27. Hao, Y.; Fang, P.; Ma, C.; White, J. C.; Xiang, Z.; Wang, H.; Zhang, Z.; Rui, Y.; Xing, B., Engineered nanomaterials inhibit Podosphaera pannosa infection on rose leaves by regulating phytohormones. *Environmental research* **2019**, *170*, 1-6, DOI 10.1016/j.envres.2018.12.008
- 28. Elmer, W. H.; Ma, C.; White, J. C., Nanoparticles for Plant Disease Management. *Current Opinion in Environmental Science & Health* **2018**, DOI 10.1016/j.coesh.2018.08.002
- 29. Datnoff, L. E.; Elmer, W. H.; Huber, D. M., *Mineral nutrition and plant disease*. American Phytopathological Society (APS Press): 2007.
- 30. Römheld, V.; Marschner, H., Function of micronutrients in plants. Micronutrients in

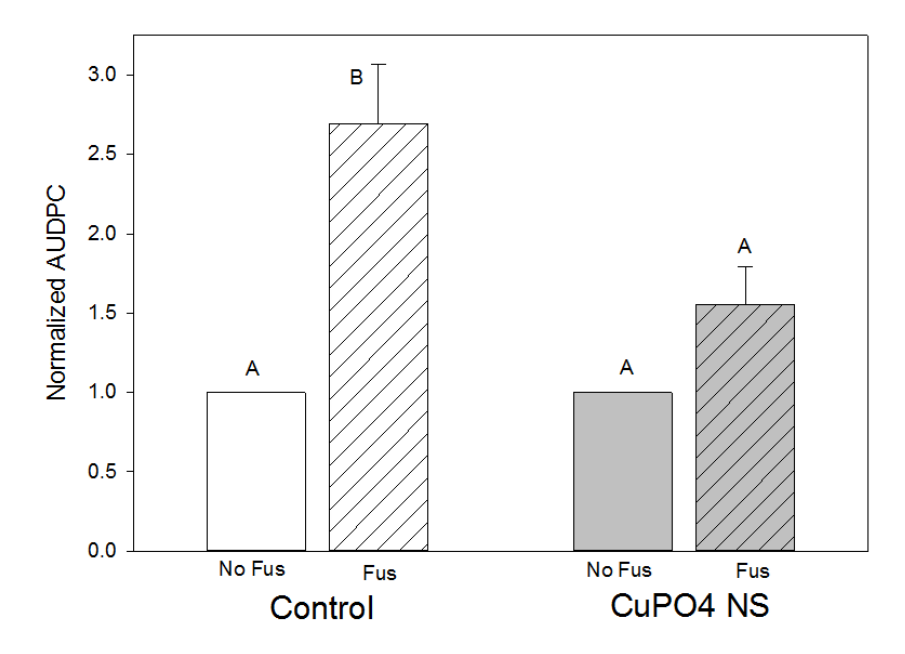
agriculture 1991, (micronutrientsi2), 297-328.

- 31. Leeper, G., Factors affecting availability of inorganic nutrients in soils with special reference to micronutrient metals. *Annual Review of Plant Physiology* **1952**, *3* (1), 1-16.
- 32. Bukovac, M.; Wittwer, S., Absorption and mobility of foliar applied nutrients. *Plant physiology* **1957**, *32* (5), 428.
- 33. Reuveni, R.; Reuveni, M., Foliar-fertilizer therapy—a concept in integrated pest management. *Crop protection* **1998**, *17* (2), 111-118, DOI 10.1016/S0261-2194(97)00108-7
- 34. Adisa, I. O.; Reddy Pullagurala, V. L.; Rawat, S.; Hernandez-Viezcas, J. A.; Dimkpa,
- C. O.; Elmer, W. H.; White, J. C.; Peralta-Videa, J. R.; Gardea-Torresdey, J. L., Role of cerium compounds in Fusarium wilt suppression and growth enhancement in tomato (Solanum lycopersicum). *Journal of agricultural and food chemistry* **2018**, *66* (24), 5959-5970, DOI 10.1021/acs.jafc.8b01345
- 35. Wang, Z.; Xie, X.; Zhao, J.; Liu, X.; Feng, W.; White, J. C.; Xing, B., Xylem-and phloem-based transport of CuO nanoparticles in maize (Zea mays L.). *Environmental science & technology* **2012**, *46* (8), 4434-4441, DOI 10.1021/es204212z

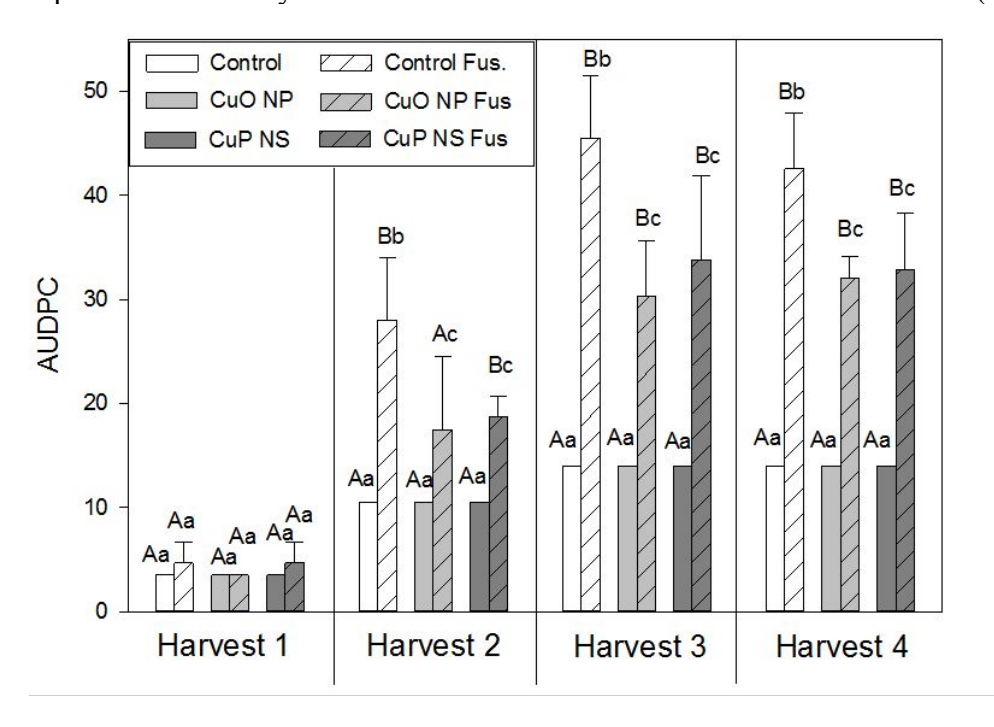


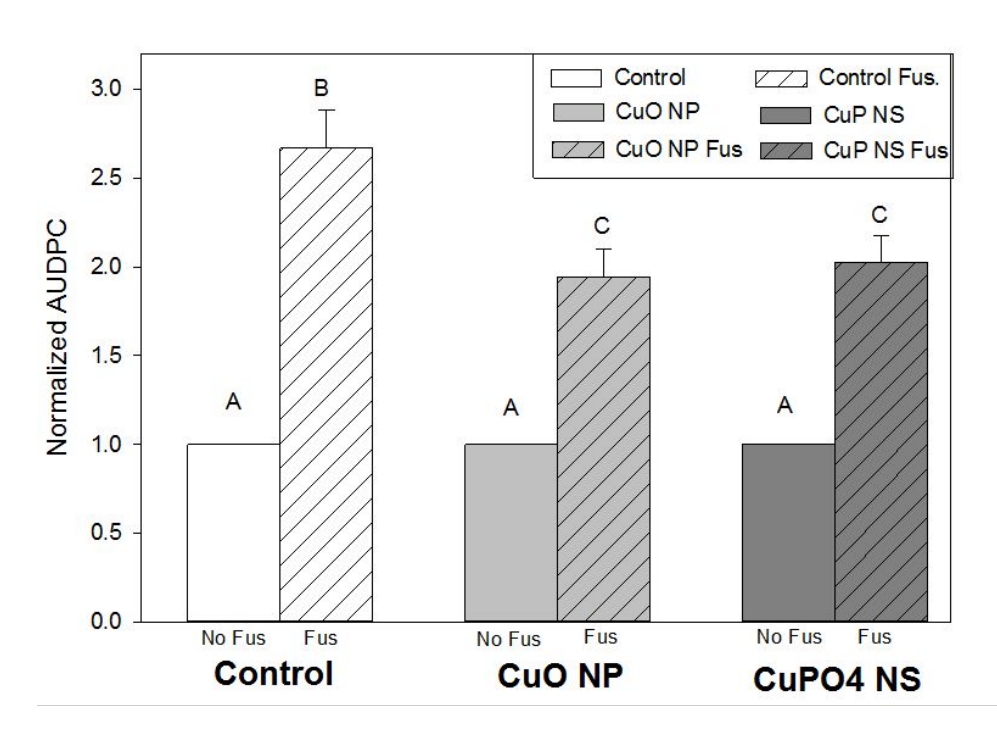
**Figure 2.** Disease progress (AUDPC) of Fusarium infection in tomato at harvests taken 7, 14, or 21 d after transplanting to infested media (A; top) or across all harvests (B; bottom) as a function of Cu<sub>3</sub>(PO<sub>4</sub>)<sub>2</sub>•3H<sub>2</sub>O nanosheet amendment. Within a harvest, bars with different letters are significantly different (one-way ANOVA with a Student Newman-Keuls multiple comparison test).



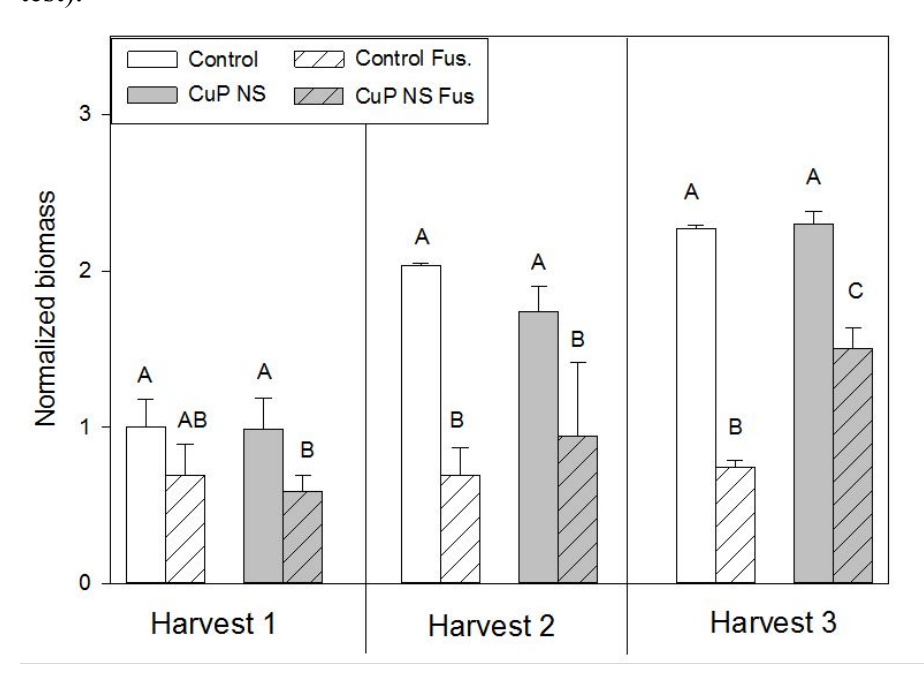


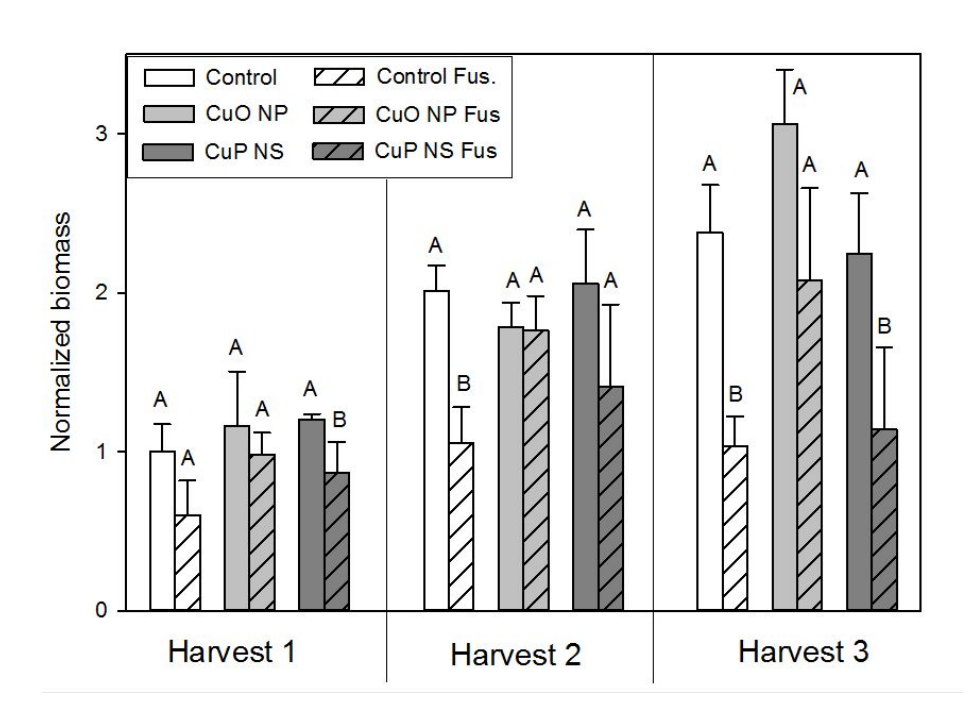
**Figure 3.** Disease progress (AUDPC) of Fusarium infection in tomato at harvests taken 7, 14, 21 or 28 d after transplanting to infested media (A; top) or across all harvests (B; bottom) as a function of CuO NP or Cu<sub>3</sub>(PO<sub>4</sub>)<sub>2</sub>•3H<sub>2</sub>O nanosheet amendment. For A, the capital letters are the result of a t-test within each pair of treatments; infected vs non-infected. The lowercase letters represent a One-way ANOVA across all 6 treatments within each harvest (also for B).



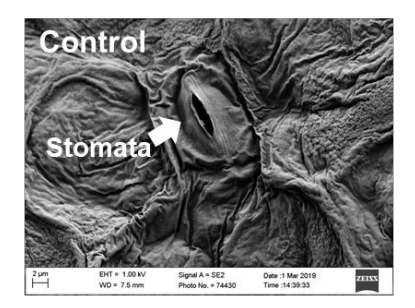


**Figure 4.** A (top-) Impact of Fusarium infection and Cu<sub>3</sub>(PO<sub>4</sub>)<sub>2</sub>•3H<sub>2</sub>O nanosheet amendment on the wet biomass of tomato harvested 7, 14, and 21 d after transplanting to infested media. Within a harvest, bars with different letters are significantly different (One-way ANOVA with a Student Newman-Keuls multiple comparison test). B (bottom)- Impact of Fusarium infection, CuO NPs or Cu<sub>3</sub>(PO<sub>4</sub>)<sub>2</sub>•3H<sub>2</sub>O nanosheet amendment on the wet biomass of tomato harvested 7, 14, and 21 d after transplanting to infested media. Within a harvest, bars with different letters are significantly different (One-way ANOVA with a Student Newman-Keuls multiple comparison test).





**Figure 5.** SEM micrographs showing the interaction between engineered nanomaterials and the tomato leaf surface. The untreated control is shown next to  $Cu_3(PO_4)_2 \bullet 3H_2O$  and  $CuO\ NP$  treatment right after exposure (0 days) and after a 7-day incubation period. The nanomaterials are circled in red for clarity.



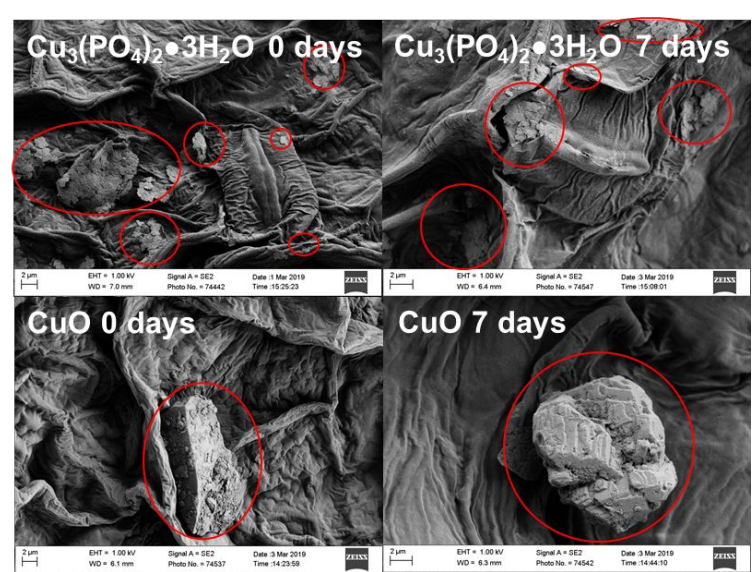
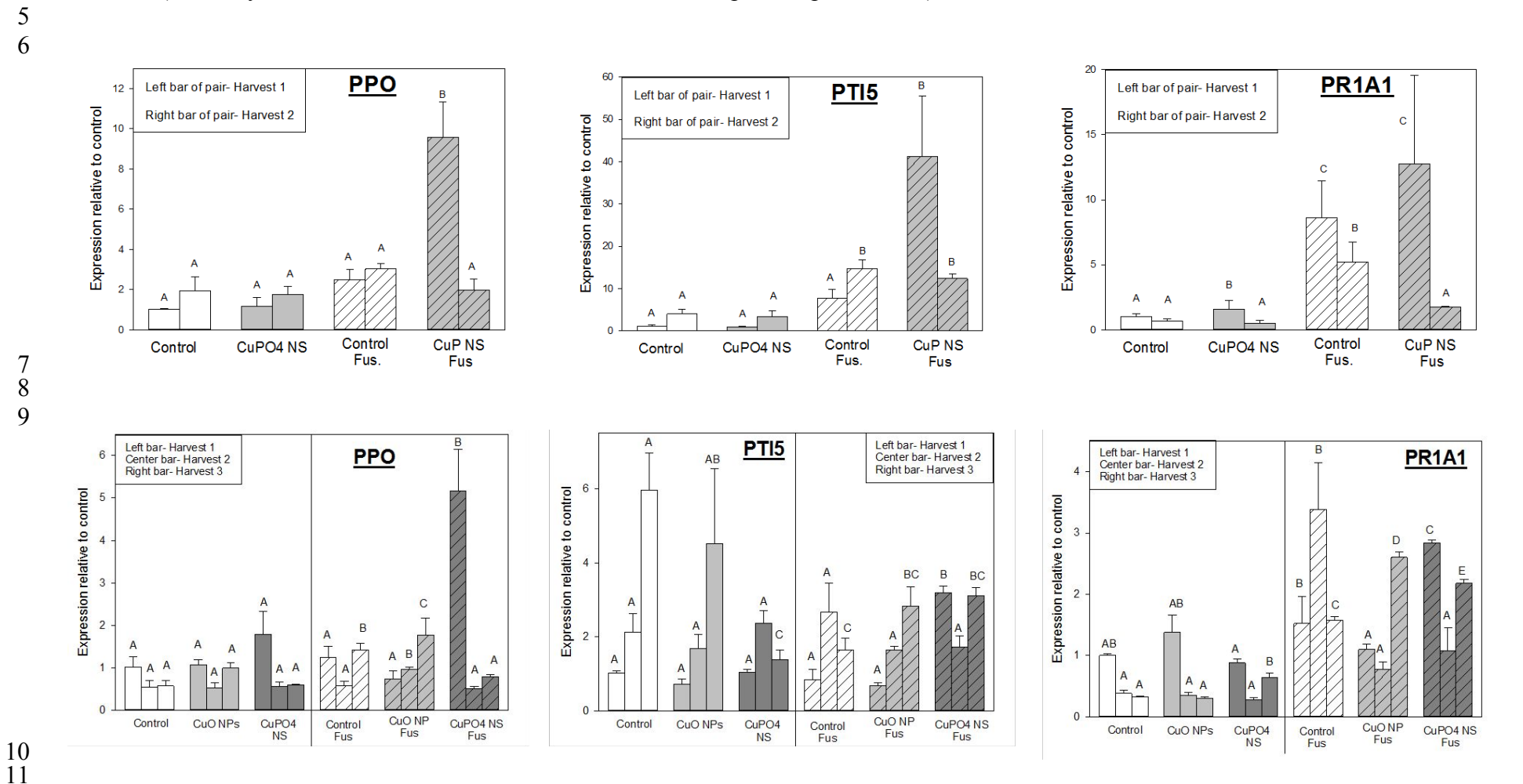


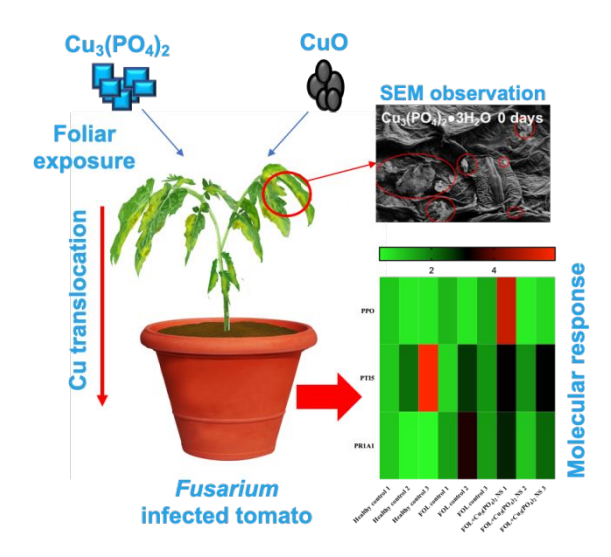
 **Figure 6.** Relative transcriptional response of 3 plant defense genes (PPO, PTI5, PR1A1) in the roots of plants 7 or 14 (A, top row) or 7, 14, or 21 d (B, bottom row) after transplanting to Fusarium infested media as a function of nanosheets or CuO NPs treatment. Across treatments (4 for A, 6 for B) but within a harvest (i.e., at a specific time point), bars with different letters are significantly different (One-way ANOVA with a Student Newman-Keuls multiple comparison test).



# For Table of Contents Use Only

#### **Synopsis**

Nanoscale Cu properties differentially altered the expression of plant pathogenesis-related genes, effectively suppressing disease and increasing growth.



**TOC Art**